

## Towards the Detection of Aircraft Icing Conditions Using Operational Dual-polarimetric Radar

Scott Ellis<sup>1\*</sup>, David Serke<sup>1</sup>, John Hubbert<sup>1</sup>, David Albo<sup>1</sup>, Andrew Weekly<sup>1</sup>,  
 Marcia Politovich<sup>1</sup>, Andrew Gaydos<sup>1</sup>, Daniel Adriaansen<sup>1</sup>, Earle R. Williams<sup>2</sup>, David J. Smalley<sup>2</sup>, and Michael F.  
 Donovan<sup>2</sup>

1. National Center for Atmospheric Research,  
 2. MIT Lincoln Laboratory

## 1. Introduction

The goal of this study is to develop an Icing Hazard Level Algorithm (IHLA) that utilizes dual-polarization radar data and output from an operational numerical weather prediction model. This work is motivated by the upcoming dual-polarization upgrade to the NEXRAD network. The IHLA algorithm is a modular design consisting of melting level detection, temperature profile adjustment and currently 3 icing condition detection modules.

The detection of super cooled liquid water (SLW), and thus inflight icing conditions, by radar alone is difficult. The liquid drops are typically quite small ( $< 50 \mu\text{m}$  in diameter) and have correspondingly low reflectivity values. If the drops are mixed with ice crystals (i.e., mixed-phase conditions), the ice crystals can dominate the backscatter radar signatures due to their generally larger size. Additionally, irregular, randomly-oriented ice crystals and small liquid drops are both characterized by  $Z_{\text{dr}}$  (differential reflectivity) and  $K_{\text{dp}}$  (specific differential phase) near zero. Thus, discrimination of SLW (a possible icing hazard) and ice crystals is challenging.

Recently, Ikeda et al. (2009) developed a freezing drizzle detection algorithm for the NEXRAD radars that was based in large part on various metrics of spatial texture of reflectivity. They hypothesized that clouds producing drizzle at the surface exhibited smoother reflectivity textures than those producing snow. They used this idea to discriminate between these two particle classes. The study showed reasonable success; approximately 70% of their observed drizzle cases were correctly identified. Plummer et al. (2010) have recently made similar type discriminations from comparisons of aircraft observations (particle probes) and S-band (NSF's S-Pol) radar data from a field campaign in northern Italy. They examined histograms of  $Z_{\text{dr}}$  and  $K_{\text{dp}}$  and concluded that:

- 1) the mean values of  $K_{\text{dp}}$  and  $Z_{\text{dr}}$  were greater in regions of ice-only as compared to mixed-phase (supercooled liquid and ice particles); and
- 2) the variance of  $Z_{\text{dr}}$  and  $K_{\text{dp}}$  were also greater in regions of ice-only as compared to mixed-phase.

Williams et al. (2011) showed that icing conditions can be detected "indirectly" with polarimetric data by inferring the microphysical processes that produce SLW. The idea is that these microphysical processes may yield precipitation particles with polarimetric signatures that suggest the existence of SLW. Williams et al. (2011) describe the microphysical processes and include a list of the relevant literature. The central idea is that different types of ice crystals form under the conditions of 1) ice saturation (no SLW) and 2) water saturation (SLW). Laboratory experiments and experimental measurements show that 1) supports pristine ice crystal growth such as plates and columns which have a relatively large fraction of ice to air. Under 2), dendrites grow, possibly with riming. The pristine type ice crystals that grow via vapor deposition are usually characterized by lower reflectivity values but can possess very high  $Z_{\text{dr}}$  values ( $> 5 \text{ dB}$ ). The dendrites produced by the presence of SLW are typically less anisotropic, less dense (lower fraction of ice to air) but their growth is quite rapid and the ice particles are typically much larger than the ice particles due to 1). Very generally, the polarimetric signatures of 2) are higher reflectivity values than 1) and large  $Z_{\text{dr}}$  but lower than 1). The  $K_{\text{dp}}$  signatures of 1) and 2) overlap since  $K_{\text{dp}}$  is a function of the bulk density of the particles and their shape and orientation.

The studies of Ikeda et al. (2009), Plummer et al. (2010) and Williams et al. (2011) focus on distinct conditions in which SLW is found and exhibit distinct polarimetric radar signatures. In order to apply the concepts outlined by the three studies, the IHLA has a modular design that will contain three fuzzy logic classifier modules based on the

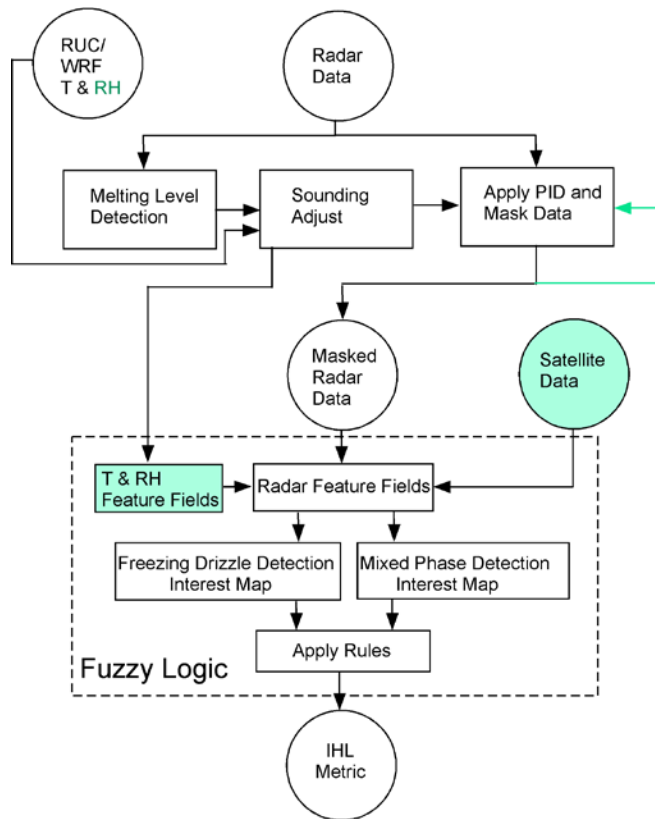
\* Corresponding Author: Scott Ellis, NCAR EOL/RSF, PO Box 3000 Boulder CO, 80307,  
[sellis@ucar.edu](mailto:sellis@ucar.edu), (303) 497-2076

results of the studies. Currently the output of each fuzzy logic module is a yes or no icing detection field. The final output is a combined icing detection product that indicates icing in a region if any of the three modules identifies icing there.

The IHLA also includes a freezing level detection algorithm (FZLA) and an implementation of the particle identification algorithm (PID) of Vivekanandan et al. (1999).

## 2. Icing Hazard Level Algorithm

The inputs to IHLA are radar and Numerical Weather Prediction (NWP) model data (Fig. 1). The Rapid Update Cycle (RUC) model was used in algorithm development; this was replaced in May 2012 with the Weather Research and Forecast Rapid Refresh (WRF-RAP) model.



The Open Radar Products Generator (ORPG) currently ingests temperature and relative humidity profiles from the NWP model. The current IHLA only uses temperature. The differences between RUC and WRF-RAP outputs were examined to prepare their Current and Forecast Icing Product (CIP and FIP) algorithms for the transition. Significant differences were not found in the temperature field. When input into the IHLA, the radar data are assumed to have been processed with an algorithm such as CMD (Clutter Mitigation Decision; Hubbert et al., 2009) and a clutter filter such as GMAP (Gaussian Model Adaptive Processing), which are used by NEXRAD.

After inputting the data, the IHLA estimates the freezing (melting) level using radar plan position indicator (PPI) data with the Freezing Level Algorithm (FZLA). The FZLA takes advantage of the radar data signatures within the freezing level, namely: increased values reflectivity ( $Z$ ) and  $Z_{dr}$  as well as decreased values of correlation coefficient ( $\rho_{hv}$ ). These radar signatures appear as ‘rings’ in the PPI data. For each elevation angle, FZLA identifies heights associated the rings in  $Z$ ,  $Z_{dr}$  and  $\rho_{hv}$ , combines the three rings into a single output and performs smoothing and clumping on the resulting

Figure 1: High-level diagram of the IHLA. Green-shaded features are not used in the current IHLA but the architecture allows for these in future versions.

ring. The ring heights found at different elevation angles are then combined through building a two-dimensional histogram to find a best estimate for the radar volume. The FZLA does not always find a freezing level, for example, if the temperature is below freezing at all levels above the surface. Details of FZLA can be found in Albo et al. (2010).

The temperature profile, or sounding, is adjusted using the freezing level found by FZLA if applicable. The PID of Vivekanandan et al. (1999) is run on the radar data using the adjusted sounding and the results are used to mask the data so that the IHLA is only applied in regions of potential icing conditions.

The masked radar data are sent to the fuzzy logic icing detection modules. The two modules currently implemented are a modified version of the Ikeda et al. (2009)-based NEXRAD Drizzle Detection Algorithm (MNDDA, referred to as FRZDRZ within IHL) and a Supercooled Liquid Water Algorithm (SLWA) based on Plummer et al. (2010). The third icing detection module based on Williams et al. (2011) is under development and testing and planned to be implemented in IHLA in the future. It is important to keep in mind that there are vastly different microphysical

cloud processes that result in the type of in-flight icing conditions described by these investigators. A radar-based icing detection algorithm needs to have the flexibility to differentiate these conditions based on the radar signatures induced by the atmospheric phenomena. The modular design of the IHLA facilitates this flexibility by allowing modules designed to identify new icing conditions to be incorporated, tested and implemented.

### 3. Results

In this section we first examine the result of the IHLA algorithm in its current form with the two fuzzy logic icing detection modules that have been implemented to date – MNDDA and SLWA. Second, we present a case study for the proto-type implementation of the third icing detection module based on Williams et al. (2011), referred to as the High  $Z_{dr}$  Algorithm (HZDRA) module. The HZDRA is under development and needs further verification. Once verified, the HZDRA detection module will be added to the IHLA algorithm.

#### 3.1 IHLA Results

In a collaborative effort with NASA, the NIRSS (NASA Icing Remote Sensing System) was brought from NASA Glenn Research Center in Cleveland, Ohio, to the Front Range of Colorado for the period of December 2010 to June 2011. NIRSS consists of a vertically-pointing Doppler  $K_a$ -band radar, a multichannel microwave radiometer and a laser ceilometer (Reehorst et al., 2006). NIRSS was deployed at the NOAA-owned Platteville, CO field site, which is close to the CSU-CHILL S-Band radar (Brunkow et al., 2000) and is conveniently located under the flight path of aircraft arriving and departing from Denver International Airport (DEN, see Fig. 6 and title page photograph). NIRSS measurements and voice pilot reports (PIREPs) were used to indicate whether or not icing conditions existed. Twice-daily meteorological balloon soundings from Denver and surface observations from the area were also used for case study analyses. The CSU-CHILL and NIRSS collected twenty-two cases during the field experiment.

Figure 2 shows the radiometer- measured integrated liquid water (ILW) at zenith from the NIRSS site for 15 and 16 December. For this case, significant ILW, defined by values  $> 0.1$  mm, only exist from 2350 UTC on the 15<sup>th</sup> until about 0110 UTC on the 16<sup>th</sup>. During this time positive icing PIREPs existed along with the significant ILW. These PIREPs occurred near the time of maximum ILW and are indicated by the black vertical line in Figure 2.

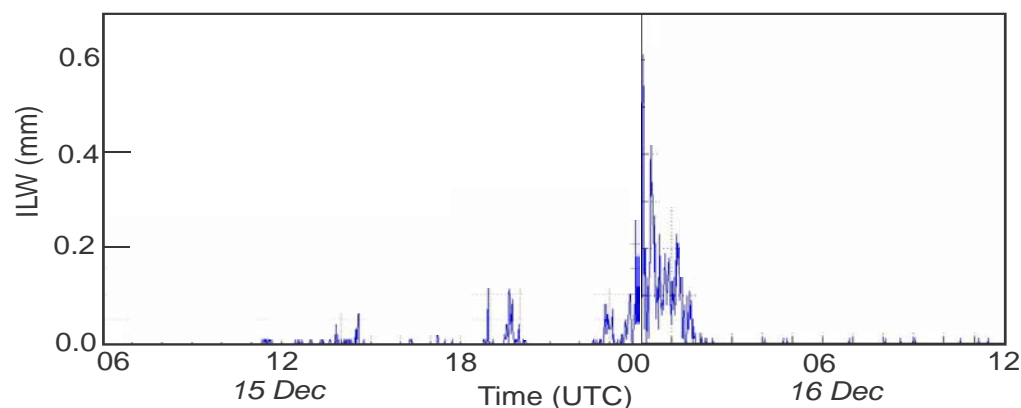


Figure 2. Time series of NIRSS radiometer ILW for 15 - 16 December 2010.

Figure 3 shows the IHLA results using CSU-CHILL data for 2251 UTC at 2.5 and 4.5° elevation angles. At this time the NIRSS radiometer measured IWL was very low at 0.05 mm indicating no icing. The IHLA resulted in a value of 0.0 over the NIRSS site indicating no icing was detected.

By 2351 UTC on 15 December, the NIRSS radiometer was beginning to detect ILW  $> 0.1$  mm. Larger areas of IHL=yes values are located close to NIRSS in both the upper and lower elevations (Fig. 4), but the NIRSS profile is actually located in a gap in CSU-CHILL radar reflectivity.

This example illustrates an important limitation of the IHLA algorithm and any radar-based icing detection system. The SLW responsible for the ILW signature measured by NIRSS were below the minimum detectable level of the

radar for the range (~ 30 km in this case). Even though the CSU-CHILL, and the NEXRADS, are powerful and highly sensitive radars, they may not be able to detect all of the clouds constituting an icing hazard.

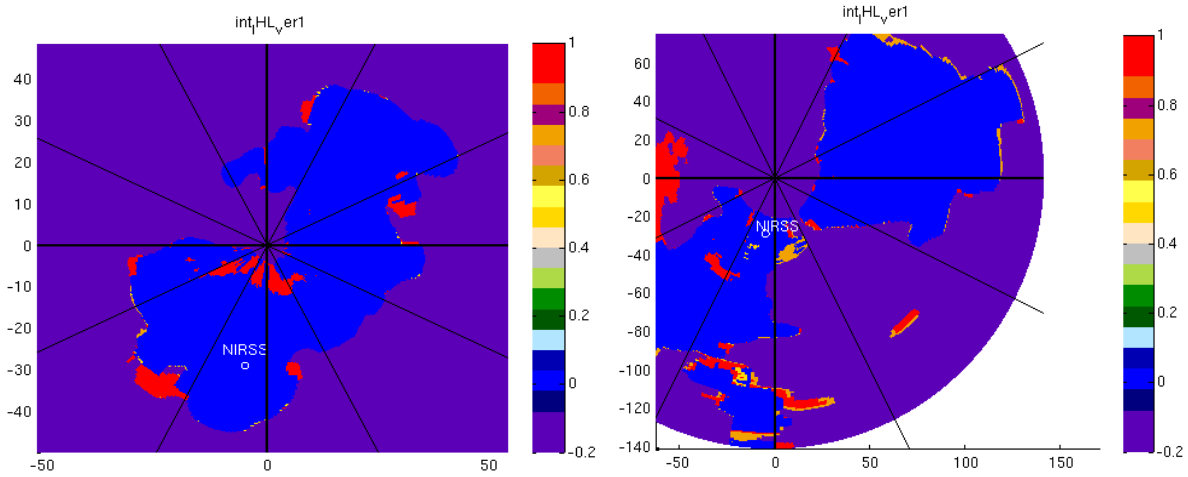


Figure 3. PPI plot of IHLA in-flight icing hazard index [unitless, scaled -0.1 to 1] for 2.5° (left) and 4.5° (right) elevations derived from CSU-CHILL radar at 2251 UTC on 15 December 2010.

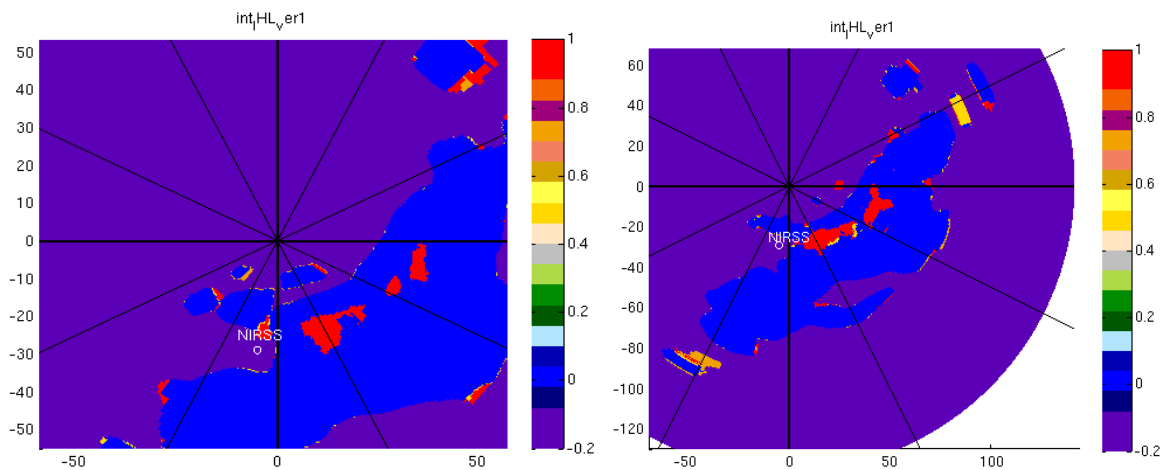


Figure 4. for Fig. 3 except at 2351 UTC 15 December 2010.

### 3.2 HZDRA Results

For the case of 30 December 2010, an elevated layer of  $Z_{dr}$  between 1 and 3 dB with reflectivity values of 10 - 30 dBZ became evident at 1730 UTC and persisted for about two hours. The NIRSS radiometer measured periods of high ILW as well as periods of insignificant ILW. The reflectivity and  $Z_{dr}$  values of icing case generally fit the pattern of water saturation suggested by Williams et al. (2011) indicating mixed-phase conditions. Since these conditions can be transient for a number of reasons, it may not be surprising that the NIRSS system measured periods with both significant ILW and close to none.

At about 17:30 UTC the NIRSS radiometer measured ILW of 0.12 mm and a PIREP was logged nearby at that time. Neither the SLWA nor the MNDDA identified potential icing conditions characterized by high  $Z_{dr}$  because they are tuned to detect different microphysical conditions with different radar signatures. In order to identify the mixed phase conditions suggested by Williams et al. (2011), a new module needs to be added to the IHLA. Figure 5 shows PPI plots of reflectivity and  $Z_{dr}$  for 30 December at 1729 UTC at an elevation angle of 0.5°. There is a layer evident, although somewhat intermittent, of elevated  $Z_{dr}$  with reflectivity values near 10 dBZ between 30 and 60 km range from CSU-CHILL.

A prototype fuzzy logic module has been designed to take advantage of the high  $Z_{dr}$  signatures associated with these mixed phase signatures called the High ZDR Algorithm (HZDRA). Figure 6 shows the output of the HZDRA for the 30 December case at 1729 UTC at  $0.5^\circ$  elevation angle (same as shown in Figure 42). The output identifies an icing risk associated with the layer of high  $Z_{dr}$  and reflectivity around 10 dBZ in a ring between 30- and 60-km range. The icing likelihood is high over the NIRSS site, where ILW values were around 0.13 mm.

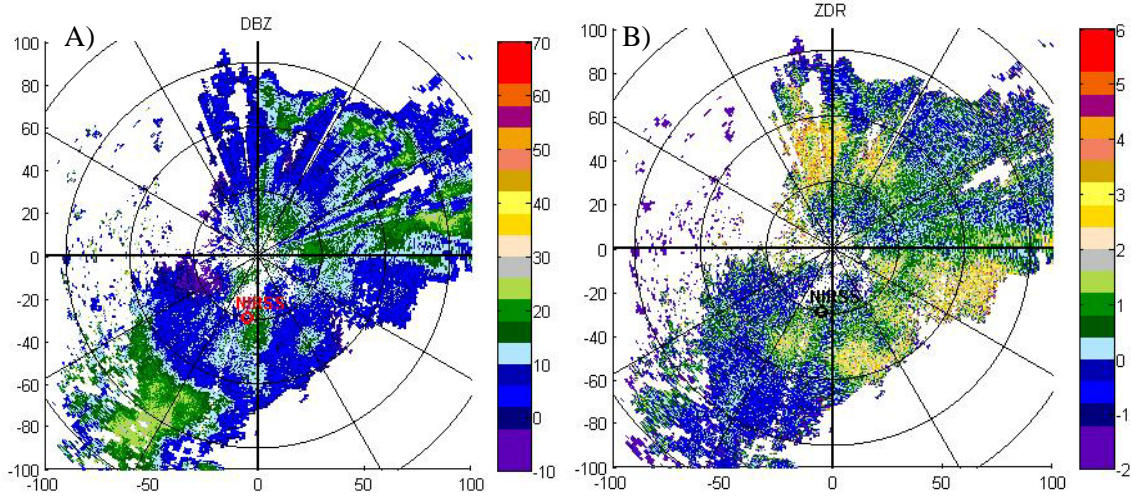


Figure 5: PPI plots of reflectivity A) and  $Z_{dr}$  B) from December 30<sup>th</sup> 2010 at 17:29 UTC. The NIRSS site is located at  $195^\circ$  azimuth and 30 km range.

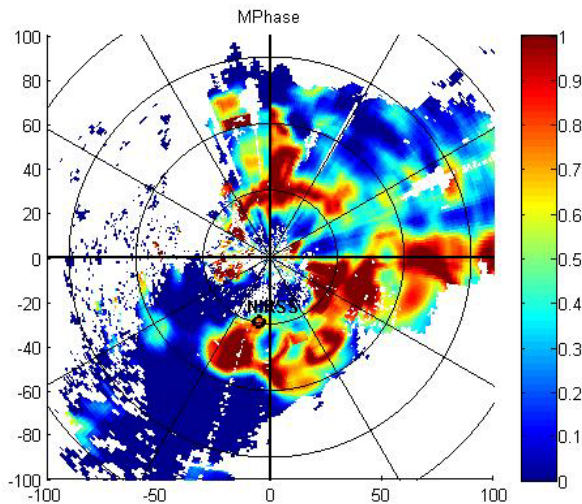


Figure 5:  $0.5^\circ$  elevation PPI of the output of the preliminary HZDRA on 30 December at 1729 UTC.

## 5. Acknowledgements

This work was sponsored by the Federal Aviation Administration under Air Force Contract No. FA8721-05-C-0002. Opinions, interpretations, conclusions, and recommendations are those of the authors and are not necessarily endorsed by the United States Government.

The National Center for Atmospheric Research is sponsored by the National Science Foundation. Any opinions, findings and conclusions or recommendations expressed in this publication are those of the author(s) and do not necessarily reflect the views of the National Science Foundation.

## 4. Future Work

This results of the modular designed IHLA presented here are encouraging, but are considered preliminary. Several improvements to the algorithm are planned. Some of these include redesigning the FZLA to operate on azimuth increments; using FZLA to identify  $Z_{dr}$  bands above the freezing level that may indicate icing following Williams et al. (2011); introducing humidity and temperature as variables into the fuzzy logic modules; conducting operational tests on dual-pol upgraded NEXRAD radars; and combining IHLA output with existing icing products such as CIP (Current Icing Product, see Bernstein et al., 2006).

## 6. References

- Albo D., S. Ellis, M. Dixon, A. Weekley, M. Politovich, G. Cunning and J. C. Hubbert, 2010: Icing Hazard Level Detection: Final Report 2010. Final Report to MIT Lincoln Laboratories, 30 Jun 2010.
- Bernstein, B.C., F. McDonough, M.K. Politovich, B.G. Brown, T.P. Ratvasky, D.R. Miller, C.A. Wolff and G. Cunning, 2005: Current Icing Potential: Algorithm Description and Comparison with Aircraft Observations. *J. Appl. Meteor.*, **44**, No. 7 (July), 969-986.
- Brunkow, D., Bringi, V. N., Kennedy, P, Rutledge, S., Chandrasekar, V., Mueller, E. and Bowie, R., "A description of the CSU-CHILL National Radar Facility", *J. Atmos. Ocean. Tech*, **17**, Issue 12, pp. 1596-1608, 2000. Hogg, D.C., F.O. Guiraud, J.B. Snider, M.T. Decker and E.R. Westwater, 1983: A steerable dual-channel microwave radiometer for measurements of water vapor and liquid water in the troposphere. *J. Climate Appl. Meteor.*, **22**, 789-806.
- Hubbert, J.C., M. Dixon, S.M. Ellis, and G. Meymaris, 2009: Weather Radar Ground Clutter. Part I: Identification, Modeling, and Simulation. *J. Atmos. Oceanic Technol.*, **26**, 1165-1180.
- Ikeda, K., Rasmussen, R., Brandes, E. and McDonough, F., 2008: Freezing drizzle detection with WSR-88D radars", *J. Appl. Meteor. Climatol*, **48**, 41-60.
- Plummer, D.M., S. Goeke, R.M. Rauber and L. DiGirolamo, 2010: Discrimination of mixed-versus ice-phase clouds using dual-polarization radar with application to detection of aircraft icing regions. *J. Appl. Meteor. Clim.*, **49**, 920 – 935.
- Reehorst, A., Politovich, M. K., Zednik, S., Isaac, G. A., & Cober, S., Progress in the Development of Practical Remote Detection of Icing Conditions (NASA/TM 2006-214242). NASA, 2006.
- Serke, D.J., J., Hubbert, S. Ellis, A. Reehorst, P. Kennedy, D. Albo, A. Weekley and M. Politovich, 2011: The winter 2010 FRONT/NIRSS in-flight icing detection field campaign. AMS 35<sup>th</sup> Conf. on Radar Meteorology, Pittsburgh, PA, 26-30 September. Available online.
- Vivekanandan, J., S.M. Ellis, R. Oye, D. S. Zrnich, A. V. Ryzhkov and J. Straka, 1999: Cloud Microphysics Retrieval Using S-band Dual-Polarization Radar Measurements. *Bull. Amer. Meteor. Soc.*, **80**, 381-388.
- Williams, E.R., D. J. Smalley, M. F. Donovan, R. G. Hallowell, K. T. Hood, B. J. Bennett, R. Evaristo, A. Stepanek, T. Bals-Elsholz, J. Cobb, and J. M. Ritzman, 2011: [Dual polarization radar winter storm studies supporting development of NEXRAD-based aviation hazard products](#). AMS 35<sup>th</sup> Conf. on Radar Meteorology, Pittsburgh, PA, 26-30 September.